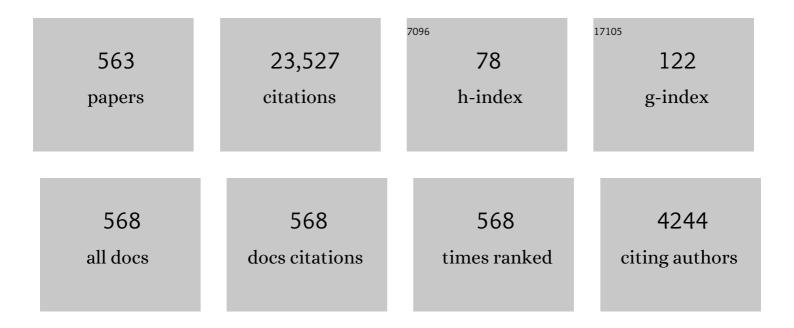
List of Publications by Year in descending order

Source: https://exaly.com/author-pdf/3113532/publications.pdf Version: 2024-02-01



#	Article	lF	CITATIONS
1	The physics basis for ignition using indirect-drive targets on the National Ignition Facility. Physics of Plasmas, 2004, 11, 339-491.	1.9	1,618
2	Point design targets, specifications, and requirements for the 2010 ignition campaign on the National Ignition Facility. Physics of Plasmas, 2011, 18, .	1.9	534
3	Review of the National Ignition Campaign 2009-2012. Physics of Plasmas, 2014, 21, 020501.	1.9	515
4	Observations of Plasmons in Warm Dense Matter. Physical Review Letters, 2007, 98, 065002.	7.8	426
5	Symmetric Inertial Confinement Fusion Implosions at Ultra-High Laser Energies. Science, 2010, 327, 1228-1231.	12.6	321
6	Progress towards ignition on the National Ignition Facility. Physics of Plasmas, 2013, 20, .	1.9	259
7	Burning plasma achieved in inertial fusion. Nature, 2022, 601, 542-548.	27.8	233
8	Demonstration of Spectrally Resolved X-Ray Scattering in Dense Plasmas. Physical Review Letters, 2003, 90, 175002.	7.8	227
9	Onset of Hydrodynamic Mix in High-Velocity, Highly Compressed Inertial Confinement Fusion Implosions. Physical Review Letters, 2013, 111, 085004.	7.8	215
10	Dante soft x-ray power diagnostic for National Ignition Facility. Review of Scientific Instruments, 2004, 75, 3759-3761.	1.3	204
11	High-energy Kα radiography using high-intensity, short-pulse lasers. Physics of Plasmas, 2006, 13, 056309.	1.9	193
12	MeasuringEandBFields in Laser-Produced Plasmas with Monoenergetic Proton Radiography. Physical Review Letters, 2006, 97, 135003.	7.8	192
13	Ultrafast X-ray Thomson Scattering of Shock-Compressed Matter. Science, 2008, 322, 69-71.	12.6	176
14	Theoretical model of x-ray scattering as a dense matter probe. Physical Review E, 2003, 67, 026412.	2.1	168
15	2D X-Ray Radiography of Imploding Capsules at the National Ignition Facility. Physical Review Letters, 2014, 112, 195001.	7.8	154
16	Observation of Megagauss-Field Topology Changes due to Magnetic Reconnection in Laser-Produced Plasmas. Physical Review Letters, 2007, 99, 055001.	7.8	151
17	Probing warm dense lithium by inelastic X-ray scattering. Nature Physics, 2008, 4, 940-944.	16.7	148
18	The experimental plan for cryogenic layered target implosions on the National Ignition Facility—The inertial confinement approach to fusion. Physics of Plasmas, 2011, 18, .	1.9	148

#	Article	IF	CITATIONS
19	X-Ray Thomson-Scattering Measurements of Density and Temperature in Shock-Compressed Beryllium. Physical Review Letters, 2009, 102, 115001.	7.8	147
20	Finite temperature dense matter studies on next-generation light sources. Journal of the Optical Society of America B: Optical Physics, 2003, 20, 770.	2.1	146
21	Inertially confined fusion plasmas dominated by alpha-particle self-heating. Nature Physics, 2016, 12, 800-806.	16.7	144
22	Threeâ€dimensional simulations of Nova high growth factor capsule implosion experiments. Physics of Plasmas, 1996, 3, 2070-2076.	1.9	143
23	Metrics for long wavelength asymmetries in inertial confinement fusion implosions on the National Ignition Facility. Physics of Plasmas, 2014, 21, .	1.9	140
24	Multiphoton ionization of the noble gases by an intense1014-W/cm2dye laser. Physical Review A, 1988, 37, 747-760.	2.5	136
25	Hot-Spot Mix in Ignition-Scale Inertial Confinement Fusion Targets. Physical Review Letters, 2013, 111, 045001.	7.8	135
26	Capsule implosion optimization during the indirect-drive National Ignition Campaign. Physics of Plasmas, 2011, 18, .	1.9	131
27	Indirect-drive noncryogenic double-shell ignition targets for the National Ignition Facility: Design and analysis. Physics of Plasmas, 2002, 9, 2221-2233.	1.9	127
28	Implosion dynamics measurements at the National Ignition Facility. Physics of Plasmas, 2012, 19, .	1.9	125
29	Development and characterization of a pair of 30–40 ps xâ€ray framing cameras. Review of Scientific Instruments, 1995, 66, 716-718.	1.3	118
30	Neutron spectrometry—An essential tool for diagnosing implosions at the National Ignition Facility (invited). Review of Scientific Instruments, 2012, 83, 10D308.	1.3	117
31	First High-Convergence Cryogenic Implosion in a Near-Vacuum Hohlraum. Physical Review Letters, 2015, 114, 175001.	7.8	117
32	High-density carbon ablator experiments on the National Ignition Facility. Physics of Plasmas, 2014, 21, .	1.9	116
33	National Ignition Campaign Hohlraum energetics. Physics of Plasmas, 2010, 17, .	1.9	115
34	Shock timing experiments on the National Ignition Facility: Initial results and comparison with simulation. Physics of Plasmas, 2012, 19, .	1.9	115
35	X-ray backlighting for the National Ignition Facility (invited). Review of Scientific Instruments, 2001, 72, 627-634.	1.3	110
36	A high-resolution integrated model of the National Ignition Campaign cryogenic layered experiments. Physics of Plasmas, 2012, 19, .	1.9	108

#	Article	IF	CITATIONS
37	Hot-spot mix in ignition-scale implosions on the NIF. Physics of Plasmas, 2012, 19, .	1.9	107
38	Nonresonant multiphoton ionization of noble gases: Theory and experiment. Physical Review Letters, 1988, 60, 1270-1273.	7.8	106
39	Generation of ultrashort x-ray pulses. Physical Review A, 1988, 37, 1684-1690.	2.5	106
40	Symmetry control of an indirectly driven high-density-carbon implosion at high convergence and high velocity. Physics of Plasmas, 2017, 24, .	1.9	106
41	Highâ€speed gated xâ€ray imaging for ICF target experiments (invited). Review of Scientific Instruments, 1992, 63, 4813-4817.	1.3	105
42	An overview of LLNL high-energy short-pulse technology for advanced radiography of laser fusion experiments. Nuclear Fusion, 2004, 44, S266-S275.	3.5	105
43	Observations of Continuum Depression in Warm Dense Matter with X-Ray Thomson Scattering. Physical Review Letters, 2014, 112, 145004.	7.8	105
44	Multistep redirection by cross-beam power transfer of ultrahigh-power lasers in a plasma. Nature Physics, 2012, 8, 344-349.	16.7	104
45	Symmetry tuning for ignition capsules via the symcap technique. Physics of Plasmas, 2011, 18, .	1.9	101
46	Characterizing counter-streaming interpenetrating plasmas relevant to astrophysical collisionless shocks. Physics of Plasmas, 2012, 19, .	1.9	101
47	Demonstration of High Performance in Layered Deuterium-Tritium Capsule Implosions in Uranium Hohlraums at the National Ignition Facility. Physical Review Letters, 2015, 115, 055001.	7.8	101
48	An in-flight radiography platform to measure hydrodynamic instability growth in inertial confinement fusion capsules at the National Ignition Facility. Physics of Plasmas, 2014, 21, .	1.9	98
49	Dense matter characterization by X-ray Thomson scattering. Journal of Quantitative Spectroscopy and Radiative Transfer, 2001, 71, 465-478.	2.3	96
50	Demonstration of Ignition Radiation Temperatures in Indirect-Drive Inertial Confinement Fusion Hohlraums. Physical Review Letters, 2011, 106, 085004.	7.8	96
51	Measuring symmetry of implosions in cryogenic <i>Hohlraums</i> at the NIF using gated x-ray detectors (invited). Review of Scientific Instruments, 2010, 81, 10E316.	1.3	95
52	Cryogenic thermonuclear fuel implosions on the National Ignition Facility. Physics of Plasmas, 2012, 19, .	1.9	95
53	Energy transfer between laser beams crossing in ignition hohlraums. Physics of Plasmas, 2009, 16, .	1.9	92
54	Diagnosing and controlling mix in National Ignition Facility implosion experiments. Physics of Plasmas, 2011, 18, .	1.9	92

#	Article	IF	CITATIONS
55	Probing high areal-density cryogenic deuterium-tritium implosions using downscattered neutron spectra measured by the magnetic recoil spectrometer. Physics of Plasmas, 2010, 17, .	1.9	91
56	Plasma-based studies with intense X-ray and particle beam sources. Laser and Particle Beams, 2002, 20, 527-536.	1.0	90
57	First Measurements of Hydrodynamic Instability Growth in Indirectly Driven Implosions at Ignition-Relevant Conditions on the National Ignition Facility. Physical Review Letters, 2014, 112, 185003.	7.8	90
58	The high velocity, high adiabat, "Bigfoot―campaign and tests of indirect-drive implosion scaling. Physics of Plasmas, 2018, 25, .	1.9	90
59	High-energy x-ray microscopy techniques for laser-fusion plasma research at the National Ignition Facility. Applied Optics, 1998, 37, 1784.	2.1	89
60	Radiation drive in laserâ€heated hohlraums. Physics of Plasmas, 1996, 3, 2057-2062.	1.9	88
61	Modeling and Interpretation of Nova's Symmetry Scaling Data Base. Physical Review Letters, 1994, 73, 2328-2331.	7.8	87
62	Design of inertial fusion implosions reaching the burning plasma regime. Nature Physics, 2022, 18, 251-258.	16.7	87
63	X-ray line measurements with high efficiency Bragg crystals. Review of Scientific Instruments, 2004, 75, 3747-3749.	1.3	86
64	Charged-Particle Probing of X-ray–Driven Inertial-Fusion Implosions. Science, 2010, 327, 1231-1235.	12.6	86
65	A review of laser–plasma interaction physics of indirect-drive fusion. Plasma Physics and Controlled Fusion, 2013, 55, 103001.	2.1	86
66	High-Performance Indirect-Drive Cryogenic Implosions at High Adiabat on the National Ignition Facility. Physical Review Letters, 2018, 121, 135001.	7.8	86
67	Efficient Multi-keV Underdense Laser-Produced Plasma Radiators. Physical Review Letters, 2001, 87, 275003.	7.8	85
68	Monoenergetic-Proton-Radiography Measurements of Implosion Dynamics in Direct-Drive Inertial-Confinement Fusion. Physical Review Letters, 2008, 100, 225001.	7.8	85
69	Development of nuclear diagnostics for the National Ignition Facility (invited). Review of Scientific Instruments, 2006, 77, 10E715.	1.3	84
70	Plasma Barodiffusion in Inertial-Confinement-Fusion Implosions: Application to Observed Yield Anomalies in Thermonuclear Fuel Mixtures. Physical Review Letters, 2010, 105, 115005.	7.8	84
71	Diagnosing implosion performance at the National Ignition Facility (NIF) by means of neutron spectrometry. Nuclear Fusion, 2013, 53, 043014.	3.5	84
72	Precision Shock Tuning on the National Ignition Facility. Physical Review Letters, 2012, 108, 215004.	7.8	83

#	Article	IF	CITATIONS
73	Demonstration of the shock-timing technique for ignition targets on the National Ignition Facility. Physics of Plasmas, 2009, 16, .	1.9	82
74	Development of Compton radiography of inertial confinement fusion implosions. Physics of Plasmas, 2011, 18, .	1.9	82
75	Analysis of the National Ignition Facility ignition hohlraum energetics experiments. Physics of Plasmas, 2011, 18, .	1.9	82
76	of Plasmas, 2015, 22, 056315.	1.9	82
77	Dynamic symmetry of indirectly driven inertial confinement fusion capsules on the National Ignition Facility. Physics of Plasmas, 2014, 21, .	1.9	81
78	Convergent ablator performance measurements. Physics of Plasmas, 2010, 17, .	1.9	80
79	Exploring the limits of case-to-capsule ratio, pulse length, and picket energy for symmetric hohlraum drive on the National Ignition Facility Laser. Physics of Plasmas, 2018, 25, .	1.9	79
80	First measurements of the absolute neutron spectrum using the magnetic recoil spectrometer at OMEGA (invited). Review of Scientific Instruments, 2008, 79, 10E502.	1.3	78
81	Reduced instability growth with high-adiabat high-foot implosions at the National Ignition Facility. Physical Review E, 2014, 90, 011102.	2.1	77
82	Soft x-ray power diagnostic improvements at the Omega Laser Facility. Review of Scientific Instruments, 2006, 77, 10E518.	1.3	76
83	The velocity campaign for ignition on NIF. Physics of Plasmas, 2012, 19, .	1.9	76
84	Record Energetics for an Inertial Fusion Implosion at NIF. Physical Review Letters, 2021, 126, 025001.	7.8	76
85	Carrier density dependent photoconductivity in diamond. Applied Physics Letters, 1990, 57, 623-625.	3.3	75
86	X-ray conversion efficiency of high-Z hohlraum wall materials for indirect drive ignition. Physics of Plasmas, 2008, 15, .	1.9	75
87	X-Ray Scattering Measurements of Strong Ion-Ion Correlations in Shock-Compressed Aluminum. Physical Review Letters, 2013, 110, 065001.	7.8	74
88	Plasmons in Strongly Coupled Shock-Compressed Matter. Physical Review Letters, 2010, 105, 075003.	7.8	73
89	Electronic structure measurements of dense plasmas. Physics of Plasmas, 2004, 11, 2754-2762.	1.9	72
90	Omega Dante soft x-ray power diagnostic component calibration at the National Synchrotron Light Source. Review of Scientific Instruments, 2004, 75, 3768-3771.	1.3	72

#	Article	IF	CITATIONS
91	Experiments and multiscale simulations ofÂlaser propagation through ignition-scaleÂplasmas. Nature Physics, 2007, 3, 716-719.	16.7	72
92	National Ignition Facility Laser System Performance. Fusion Science and Technology, 2016, 69, 366-394.	1.1	70
93	X-ray scattering from solid density plasmas. Physics of Plasmas, 2003, 10, 2433-2441.	1.9	69
94	Observations of Electromagnetic Fields and Plasma Flow in Hohlraums with Proton Radiography. Physical Review Letters, 2009, 102, 205001.	7.8	69
95	Diffusive, supersonic x-ray transport in radiatively heated foam cylinders. Physics of Plasmas, 2000, 7, 2126-2134.	1.9	68
96	Absolute xâ€ray power measurements with subnanosecond time resolution using type lla diamond photoconductors. Journal of Applied Physics, 1990, 68, 124-130.	2.5	66
97	The first measurements of soft x-ray flux from ignition scale <i>Hohlraums</i> at the National Ignition Facility using DANTE (invited). Review of Scientific Instruments, 2010, 81, 10E321.	1.3	66
98	Xâ€ray radiographic measurements of radiationâ€driven shock and interface motion in solid density material. Physics of Fluids B, 1993, 5, 2259-2264.	1.7	65
99	Three-Dimensional Single Mode Rayleigh-Taylor Experiments on Nova. Physical Review Letters, 1995, 75, 3677-3680.	7.8	65
100	Hohlraum Radiation Drive Measurements on the Omega Laser. Physical Review Letters, 1997, 79, 1491-1494.	7.8	65
101	Nuclear imaging of the fuel assembly in ignition experiments. Physics of Plasmas, 2013, 20, 056320.	1.9	65
102	Thomson Scattering from Inertial-Confinement-Fusion Hohlraum Plasmas. Physical Review Letters, 1997, 79, 1277-1280.	7.8	64
103	X-ray scattering measurements on imploding CH spheres at the National Ignition Facility. Physical Review E, 2016, 94, 011202.	2.1	64
104	Indirect drive ignition at the National Ignition Facility. Plasma Physics and Controlled Fusion, 2017, 59, 014021.	2.1	64
105	Modified Bell–Plesset effect with compressibility: Application to double-shell ignition target designs. Physics of Plasmas, 2003, 10, 820-829.	1.9	62
106	Progress in hohlraum physics for the National Ignition Facility. Physics of Plasmas, 2014, 21, .	1.9	62
107	Cryogenic tritium-hydrogen-deuterium and deuterium-tritium layer implosions with high density carbon ablators in near-vacuum hohlraums. Physics of Plasmas, 2015, 22, 062703.	1.9	62
108	X-Ray Scattering Measurements of Radiative Heating and Cooling Dynamics. Physical Review Letters, 2008, 101, 045003.	7.8	61

#	Article	IF	CITATIONS
109	Hydrodynamic instability growth and mix experiments at the National Ignition Facility. Physics of Plasmas, 2014, 21, .	1.9	60
110	Measurements of an Ablator-Gas Atomic Mix in Indirectly Driven Implosions at the National Ignition Facility. Physical Review Letters, 2014, 112, 025002.	7.8	60
111	Measurement of the expansion of picosecond laser-produced plasmas using resonance absorption profile spectroscopy. Physical Review Letters, 1989, 63, 1475-1478.	7.8	59
112	Hohlraum energetics scaling to 520 TW on the National Ignition Facility. Physics of Plasmas, 2013, 20, .	1.9	59
113	Integrated modeling of cryogenic layered highfoot experiments at the NIF. Physics of Plasmas, 2016, 23,	1.9	59
114	Monoenergetic proton backlighter for measuring E and B fields and for radiographing implosions and high-energy density plasmas (invited). Review of Scientific Instruments, 2006, 77, 10E725.	1.3	58
115	Hot electron measurements in ignition relevant <i>Hohlraums</i> on the National Ignition Facility. Review of Scientific Instruments, 2010, 81, 10D938.	1.3	58
116	In-Flight Measurements of Capsule Shell Adiabats in Laser-Driven Implosions. Physical Review Letters, 2011, 107, 015002.	7.8	58
117	First Observations of Nonhydrodynamic Mix at the Fuel-Shell Interface in Shock-Driven Inertial Confinement Implosions. Physical Review Letters, 2014, 112, 135001.	7.8	58
118	Improved Performance of High Areal Density Indirect Drive Implosions at the National Ignition Facility using a Four-Shock Adiabat Shaped Drive. Physical Review Letters, 2015, 115, 105001.	7.8	58
119	X-ray ablation rates in inertial confinement fusion capsule materials. Physics of Plasmas, 2011, 18, .	1.9	57
120	Imaging of high-energy x-ray emission from cryogenic thermonuclear fuel implosions on the NIF. Review of Scientific Instruments, 2012, 83, 10E115.	1.3	57
121	Assembly of High-Areal-Density Deuterium-Tritium Fuel from Indirectly Driven Cryogenic Implosions. Physical Review Letters, 2012, 108, 215005.	7.8	57
122	Detailed Measurements of a Diffusive Supersonic Wave in a Radiatively Heated Foam. Physical Review Letters, 2000, 84, 274-277.	7.8	56
123	Measurement of carbon ionization balance in high-temperature plasma mixtures by temporally resolved X-ray scattering. Journal of Quantitative Spectroscopy and Radiative Transfer, 2006, 99, 225-237.	2.3	56
124	Thin Shell, High Velocity Inertial Confinement Fusion Implosions on the National Ignition Facility. Physical Review Letters, 2015, 114, 145004.	7.8	56
125	Opacity measurements: Extending the range and filling in the gaps. Journal of Quantitative Spectroscopy and Radiative Transfer, 1997, 58, 415-425.	2.3	55
126	Energetics of Inertial Confinement Fusion Hohlraum Plasmas. Physical Review Letters, 1998, 80, 2845-2848.	7.8	55

#	Article	IF	CITATIONS
127	Multi-keV x-ray conversion efficiency in laser-produced plasmas. Physics of Plasmas, 2003, 10, 2047-2055.	1.9	55
128	Observation of High Soft X-Ray Drive in Large-Scale Hohlraums at the National Ignition Facility. Physical Review Letters, 2011, 106, 085003.	7.8	55
129	Backlighter development at the National Ignition Facility (NIF): Zinc to zirconium. High Energy Density Physics, 2013, 9, 626-634.	1.5	55
130	The relationship between gas fill density and hohlraum drive performance at the National Ignition Facility. Physics of Plasmas, 2017, 24, .	1.9	55
131	Achieving record hot spot energies with large HDC implosions on NIF in HYBRID-E. Physics of Plasmas, 2021, 28, .	1.9	55
132	Three-wavelength scheme to optimize hohlraum coupling on the National Ignition Facility. Physical Review E, 2011, 83, 046409.	2.1	54
133	X-ray driven implosions at ignition relevant velocities on the National Ignition Facility. Physics of Plasmas, 2013, 20, .	1.9	54
134	Improving ICF implosion performance with alternative capsule supports. Physics of Plasmas, 2017, 24, .	1.9	54
135	Electrical Transport Properties of Undoped CVD Diamond Films. Science, 1992, 255, 830-833.	12.6	53
136	The role of symmetry in indirectâ€drive laser fusion. Physics of Plasmas, 1995, 2, 2488-2494.	1.9	53
137	Toward a burning plasma state using diamond ablator inertially confined fusion (ICF) implosions on the National Ignition Facility (NIF). Plasma Physics and Controlled Fusion, 2019, 61, 014023.	2.1	53
138	Symmetric Inertial-Confinement-Fusion-Capsule Implosions in a Double-Z-Pinch-Driven Hohlraum. Physical Review Letters, 2002, 89, 245002.	7.8	52
139	Probing matter at Gbar pressures at the NIF. High Energy Density Physics, 2014, 10, 27-34.	1.5	52
140	Measurements of Ionic Structure in Shock Compressed Lithium Hydride from Ultrafast X-Ray Thomson Scattering. Physical Review Letters, 2009, 103, 245004.	7.8	51
141	A high-resolution two-dimensional imaging velocimeter. Review of Scientific Instruments, 2010, 81, 035101.	1.3	51
142	Capsule performance optimization in the National Ignition Campaign. Physics of Plasmas, 2010, 17, .	1.9	51
143	Suprathermal electrons generated by the two-plasmon-decay instability in gas-filled <i>Hohlraums</i> . Physics of Plasmas, 2010, 17, .	1.9	51
144	Progress toward a self-consistent set of 1D ignition capsule metrics in ICF. Physics of Plasmas, 2018, 25, .	1.9	51

#	Article	IF	CITATIONS
145	Ablation front Rayleigh–Taylor growth experiments in spherically convergent geometry. Physics of Plasmas, 2000, 7, 2033-2039.	1.9	50
146	Proof of principle experiments that demonstrate utility of cocktail hohlraums for indirect drive ignition. Physics of Plasmas, 2007, 14, 056311.	1.9	50
147	Plasma-based beam combiner for very high fluence and energy. Nature Physics, 2018, 14, 80-84.	16.7	50
148	Hotspot conditions achieved in inertial confinement fusion experiments on the National Ignition Facility. Physics of Plasmas, 2020, 27, .	1.9	50
149	2015, 22, 056314.	1.9	49
150	The role of hot spot mix in the low-foot and high-foot implosions on the NIF. Physics of Plasmas, 2017, 24, .	1.9	49
151	Ultrafast probing of magnetic field growth inside a laser-driven solenoid. Physical Review E, 2017, 95, 033208.	2.1	49
152	An analytic asymmetric-piston model for the impact of mode-1 shell asymmetry on ICF implosions. Physics of Plasmas, 2020, 27, .	1.9	49
153	X-ray probe development for collective scattering measurements in dense plasmas. Journal of Quantitative Spectroscopy and Radiative Transfer, 2006, 99, 636-648.	2.3	48
154	Observation of the Decay Dynamics and Instabilities of Megagauss Field Structures in Laser-Produced Plasmas. Physical Review Letters, 2007, 99, 015001.	7.8	48
155	X-ray conversion efficiency in vacuum hohlraum experiments at the National Ignition Facility. Physics of Plasmas, 2012, 19, 053301.	1.9	48
156	Performance of High-Convergence, Layered DT Implosions with Extended-Duration Pulses at the National Ignition Facility. Physical Review Letters, 2013, 111, 215001.	7.8	47
157	On the importance of minimizing "coast-time―in x-ray driven inertially confined fusion implosions. Physics of Plasmas, 2017, 24, .	1.9	47
158	Hydrodynamic instability growth of three-dimensional, "native-roughness―modulations in x-ray driven, spherical implosions at the National Ignition Facility. Physics of Plasmas, 2015, 22, .	1.9	46
159	X-ray shadow imprint of hydrodynamic instabilities on the surface of inertial confinement fusion capsules by the fuel fill tube. Physical Review E, 2017, 95, 031204.	2.1	46
160	Radiation-Driven Hydrodynamics of High-ZHohlraums on the National Ignition Facility. Physical Review Letters, 2005, 95, 215004.	7.8	45
161	A hardened gated x-ray imaging diagnostic for inertial confinement fusion experiments at the National Ignition Facility. Review of Scientific Instruments, 2010, 81, 10E539.	1.3	45
162	Generation and Beaming of Early Hot Electrons onto the Capsule in Laser-Driven Ignition Hohlraums. Physical Review Letters, 2016, 116, 075003.	7.8	45

#	Article	IF	CITATIONS
163	High-energy (>70 keV) x-ray conversion efficiency measurement on the ARC laser at the National Ignition Facility. Physics of Plasmas, 2017, 24, .	1.9	45
164	Observation of Saturation of Energy Transfer between Copropagating Beams in a Flowing Plasma. Physical Review Letters, 2002, 89, 215003.	7.8	44
165	Generalized x-ray scattering cross section from nonequilibrium plasmas. Physical Review E, 2006, 74, 026402.	2.1	44
166	Direct Measurement of Energetic Electrons Coupling to an Imploding Low-Adiabat Inertial Confinement Fusion Capsule. Physical Review Letters, 2012, 108, 135006.	7.8	44
167	Early-Time Symmetry Tuning in the Presence of Cross-Beam Energy Transfer in ICF Experiments on the National Ignition Facility. Physical Review Letters, 2013, 111, 235001.	7.8	44
168	Azimuthal Drive Asymmetry in Inertial Confinement Fusion Implosions on the National Ignition Facility. Physical Review Letters, 2020, 124, 145002.	7.8	44
169	Characteristics of high energy Kα and Bremsstrahlung sources generated by short pulse petawatt lasers. Review of Scientific Instruments, 2004, 75, 4048-4050.	1.3	43
170	Demonstration of Enhanced Radiation Drive in Hohlraums Made from a Mixture of High-ZWall Materials. Physical Review Letters, 2007, 98, .	7.8	43
171	Demonstration of the Density Dependence of X-Ray Flux in a Laser-Driven Hohlraum. Physical Review Letters, 2008, 101, 035001.	7.8	43
172	Lorentz Mapping of Magnetic Fields in Hot Dense Plasmas. Physical Review Letters, 2009, 103, 085001.	7.8	43
173	Temperature measurement through detailed balance in x-ray Thomson scattering. High Energy Density Physics, 2009, 5, 182-186.	1.5	43
174	Inelastic X-Ray Scattering from Shocked Liquid Deuterium. Physical Review Letters, 2012, 109, 265003.	7.8	43
175	Refraction-enhanced x-ray radiography for inertial confinement fusion and laser-produced plasma applications. Journal of Applied Physics, 2009, 105, .	2.5	42
176	Images of the laser entrance hole from the static x-ray imager at NIF. Review of Scientific Instruments, 2010, 81, 10E538.	1.3	42
177	Development of the CD Symcap platform to study gas-shell mix in implosions at the National Ignition Facility. Physics of Plasmas, 2014, 21, .	1.9	42
178	Short pulse, high resolution, backlighters for point projection high-energy radiography at the National Ignition Facility. Physics of Plasmas, 2017, 24, .	1.9	42
179	The influence of hohlraum dynamics on implosion symmetry in indirect drive inertial confinement fusion experiments. Physics of Plasmas, 2018, 25, .	1.9	42
180	Demonstration of Scale-Invariant Rayleigh-Taylor Instability Growth in Laser-Driven Cylindrical Implosion Experiments. Physical Review Letters, 2020, 124, 185003.	7.8	42

#	Article	IF	CITATIONS
181	Development of backlighting sources for a Compton radiography diagnostic of inertial confinement fusion targets (invited). Review of Scientific Instruments, 2008, 79, 10E901.	1.3	41
182	First implosion experiments with cryogenic thermonuclear fuel on the National Ignition Facility. Plasma Physics and Controlled Fusion, 2012, 54, 045013.	2.1	41
183	Mixing in ICF implosions on the National Ignition Facility caused by the fill-tube. Physics of Plasmas, 2020, 27, .	1.9	41
184	High performance imaging streak camera for the National Ignition Facility. Review of Scientific Instruments, 2012, 83, 125105.	1.3	40
185	The effect of laser pulse shape variations on the adiabat of NIF capsule implosions. Physics of Plasmas, 2013, 20, .	1.9	40
186	Stabilization of high-compression, indirect-drive inertial confinement fusion implosions using a 4-shock adiabat-shaped drive. Physics of Plasmas, 2015, 22, .	1.9	40
187	A 3D dynamic model to assess the impacts of low-mode asymmetry, aneurysms and mix-induced radiative loss on capsule performance across inertial confinement fusion platforms. Nuclear Fusion, 2019, 59, 032009.	3.5	40
188	Evidence of Three-Dimensional Asymmetries Seeded by High-Density Carbon-Ablator Nonuniformity in Experiments at the National Ignition Facility. Physical Review Letters, 2021, 126, 025002.	7.8	40
189	Resonant Multiphoton Ionization of Krypton by Intense uv Laser Radiation. Physical Review Letters, 1987, 59, 2558-2561.	7.8	39
190	Dynamics of picosecond-laser-pulse plasmas determined from the spectral shifts of reflected probe pulses. Physical Review A, 1992, 46, 5089-5100.	2.5	39
191	Inertial Confinement Fusion with Tetrahedral Hohlraums at OMEGA. Physical Review Letters, 1999, 82, 3807-3810.	7.8	39
192	Amplification of an ultrashort pulse laser by stimulated Raman scattering of a 1ns pulse in a low density plasma. Physics of Plasmas, 2007, 14, 113109.	1.9	39
193	Comparison of plastic, high density carbon, and beryllium as indirect drive NIF ablators. Physics of Plasmas, 2018, 25, .	1.9	39
194	Absolute Equation-of-State Measurement for Polystyrene from 25 to 60ÂMbar Using a Spherically Converging Shock Wave. Physical Review Letters, 2018, 121, 025001.	7.8	39
195	Multi-beam effects on backscatter and its saturation in experiments with conditions relevant to ignition. Physics of Plasmas, 2011, 18, .	1.9	38
196	Charged-particle spectroscopy for diagnosing shock ÏR and strength in NIF implosions. Review of Scientific Instruments, 2012, 83, 10D901.	1.3	38
197	A novel particle time of flight diagnostic for measurements of shock- and compression-bang times in D3He and DT implosions at the NIF. Review of Scientific Instruments, 2012, 83, 10D902.	1.3	38
198	Progress in the indirect-drive National Ignition Campaign. Plasma Physics and Controlled Fusion, 2012, 54, 124026.	2.1	38

#	Article	IF	CITATIONS
199	High-density carbon capsule experiments on the national ignition facility. Physical Review E, 2015, 91, 021101.	2.1	38
200	Resolving hot spot microstructure using x-ray penumbral imaging (invited). Review of Scientific Instruments, 2016, 87, 11E201.	1.3	38
201	Performance of indirectly driven capsule implosions on the National Ignition Facility using adiabat-shaping. Physics of Plasmas, 2016, 23, 056303.	1.9	38
202	Progress of indirect drive inertial confinement fusion in the United States. Nuclear Fusion, 2019, 59, 112018.	3.5	38
203	Diagnosing direct-drive, shock-heated, and compressed plastic planar foils with noncollective spectrally resolved x-ray scattering. Physics of Plasmas, 2007, 14, 122703.	1.9	37
204	Measurements of Radial Heat Wave Propagation in Laser-Produced Exploding-Foil Plasmas. Physical Review Letters, 1994, 73, 2055-2058.	7.8	36
205	A simple time-dependent analytic model of the P2 asymmetry in cylindrical hohlraums. Physics of Plasmas, 1999, 6, 2137-2143.	1.9	35
206	X-ray imaging techniques onZusing the Z-Beamlet laser. Review of Scientific Instruments, 2001, 72, 657-662.	1.3	35
207	Efficient, 1–100-keV x-ray radiography with high spatial and temporal resolution. Optics Letters, 2002, 27, 134.	3.3	35
208	Development of intense point x-ray sources for backlighting high energy density experiments (invited). Review of Scientific Instruments, 2004, 75, 3915-3920.	1.3	35
209	Electron-density scaling of conversion efficiency of laser energy into L-shell X-rays. Journal of Quantitative Spectroscopy and Radiative Transfer, 2006, 99, 186-198.	2.3	35
210	K-alpha conversion efficiency measurements for X-ray scattering in inertial confinement fusion plasmas. High Energy Density Physics, 2007, 3, 156-162.	1.5	35
211	Progress towards ignition on the National Ignition Facility. Nuclear Fusion, 2011, 51, 094024.	3.5	35
212	The Crystal Backlighter Imager: A spherically bent crystal imager for radiography on the National Ignition Facility. Review of Scientific Instruments, 2019, 90, 013702.	1.3	35
213	X-ray characterization of picosecond laser plasmas. Optics Communications, 1987, 63, 253-258.	2.1	34
214	Review of drive symmetry measurement and control experiments on the Nova laser system (invited). Review of Scientific Instruments, 1995, 66, 672-677.	1.3	34
215	Angular sensitivity of gated microchannel plate framing cameras. Review of Scientific Instruments, 2001, 72, 709-712.	1.3	34
216	National Ignition Facility scale hohlraum asymmetry studies by thin shell radiography. Physics of Plasmas. 2001. 8. 2357-2364.	1.9	34

#	Article	IF	CITATIONS
217	Strong coupling corrections in the analysis of x-ray Thomson scattering measurements. Journal of Physics A, 2003, 36, 5971-5980.	1.6	34
218	NIF Ignition Target Requirements, Margins, and Uncertainties: Status February 2010. Fusion Science and Technology, 2011, 59, 1-7.	1.1	34
219	Electron temperature measurements inside the ablating plasma of gas-filled hohlraums at the National Ignition Facility. Physics of Plasmas, 2016, 23, .	1.9	34
220	Symmetry control in subscale near-vacuum hohlraums. Physics of Plasmas, 2016, 23, .	1.9	34
221	Time-resolved probing of electron thermal transport in plasma produced by femtosecond laser pulses. Physical Review Letters, 1994, 72, 3823-3826.	7.8	33
222	X-ray radiography and scattering diagnosis of dense shock-compressed matter. Physics of Plasmas, 2010, 17, .	1.9	33
223	Investigation of ion kinetic effects in direct-drive exploding-pusher implosions at the NIF. Physics of Plasmas, 2014, 21, 122712.	1.9	33
224	Resonantly enhanced multiphoton ionization of krypton and xenon with intense ultraviolet laser radiation. Physical Review A, 1988, 38, 2815-2829.	2.5	32
225	Fusion neutrons from the gas–pusher interface in deuterated-shell inertial confinement fusion implosions. Physics of Plasmas, 1998, 5, 768-774.	1.9	32
226	Numerical modeling of Hohlraum radiation conditions: Spatial and spectral variations due to sample position, beam pointing, and Hohlraum geometry. Physics of Plasmas, 2005, 12, 122703.	1.9	32
227	Probing the seeding of hydrodynamic instabilities from nonuniformities in ablator materials using 2D velocimetry. Physics of Plasmas, 2018, 25, .	1.9	32
228	Enhanced energy coupling for indirectly driven inertial confinement fusion. Nature Physics, 2019, 15, 138-141.	16.7	32
229	Demonstration of time-dependent symmetry control in hohlraums by drive-beam staggering. Physics of Plasmas, 2000, 7, 333-337.	1.9	31
230	Proton radiography of dynamic electric and magnetic fields in laser-produced high-energy-density plasmas. Physics of Plasmas, 2009, 16, .	1.9	31
231	Adiabat-shaping in indirect drive inertial confinement fusion. Physics of Plasmas, 2015, 22, 052702.	1.9	31
232	Examining the radiation drive asymmetries present in the high foot series of implosion experiments at the National Ignition Facility. Physics of Plasmas, 2017, 24, .	1.9	31
233	Thermal Temperature Measurements of Inertial Fusion Implosions. Physical Review Letters, 2018, 121, 085001.	7.8	31
234	Review of hydrodynamic instability experiments in inertially confined fusion implosions on National Ignition Facility. Plasma Physics and Controlled Fusion, 2020, 62, 014007.	2.1	31

#	Article	IF	CITATIONS
235	Improved gas-filled hohlraum performance on Nova with beam smoothing. Physics of Plasmas, 1998, 5, 1927-1934.	1.9	30
236	Refraction-enhanced x-ray radiography for density profile measurements at CH/Be interface. Journal of Instrumentation, 2011, 6, P09004-P09004.	1.2	30
237	Experimental demonstration of early time, hohlraum radiation symmetry tuning for indirect drive ignition experiments. Physics of Plasmas, 2011, 18, 092703.	1.9	30
238	Hydrodynamic instability growth of three-dimensional modulations in radiation-driven implosions with "low-foot―and "high-foot―drives at the National Ignition Facility. Physics of Plasmas, 2017, 24, .	1.9	30
239	Mitigation of X-ray shadow seeding of hydrodynamic instabilities on inertial confinement fusion capsules using a reduced diameter fuel fill-tube. Physics of Plasmas, 2018, 25, .	1.9	30
240	Hohlraum-Driven High-Convergence Implosion Experiments with Multiple Beam Cones on the Omega Laser Facility. Physical Review Letters, 2002, 89, 165001.	7.8	29
241	Progress in long scale length laser–plasma interactions. Nuclear Fusion, 2004, 44, S185-S190.	3.5	29
242	First results of radiation-driven, layered deuterium-tritium implosions with a 3-shock adiabat-shaped drive at the National Ignition Facility. Physics of Plasmas, 2015, 22, .	1.9	29
243	X-ray backlit imaging measurement of in-flight pusher density for an indirect drive capsule implosion. Review of Scientific Instruments, 1997, 68, 814-816.	1.3	28
244	Hohlraum Symmetry Experiments with Multiple Beam Cones on the Omega Laser Facility. Physical Review Letters, 1998, 81, 108-111.	7.8	28
245	Symmetric inertial confinement fusion capsule implosions in a high-yield-scale double-Z-pinch-driven hohlraum on Z. Physics of Plasmas, 2003, 10, 3717-3727.	1.9	28
246	Supersonic propagation of ionization waves in an underdense, laser-produced plasma. Physics of Plasmas, 2005, 12, 063104.	1.9	28
247	Hard x-ray and hot electron environment in vacuum hohlraums at the National Ignition Facility. Physics of Plasmas, 2006, 13, 032703.	1.9	28
248	Measurement of the Adiabatic Index in Be Compressed by Counterpropagating Shocks. Physical Review Letters, 2012, 108, 175006.	7.8	28
249	Measurement of High-Pressure Shock Waves in Cryogenic Deuterium-Tritium Ice Layered Capsule Implosions on NIF. Physical Review Letters, 2013, 111, 065003.	7.8	28
250	NIF Ignition Campaign Target Performance and Requirements: Status May 2012. Fusion Science and Technology, 2013, 63, 67-75.	1.1	28
251	Measurement of Hydrodynamic Growth near Peak Velocity in an Inertial Confinement Fusion Capsule Implosion using a Self-Radiography Technique. Physical Review Letters, 2016, 117, 035001.	7.8	28
252	Developing an Experimental Basis for Understanding Transport in NIF Hohlraum Plasmas. Physical Review Letters, 2018, 121, 095002.	7.8	28

#	Article	IF	CITATIONS
253	Achromatically filtered diamond photoconductive detectors for high power soft x-ray flux measurements. Review of Scientific Instruments, 1999, 70, 656-658.	1.3	27
254	Streaked radiography measurements of convergent ablator performance (invited). Review of Scientific Instruments, 2010, 81, 10E304.	1.3	27
255	Impeding Hohlraum Plasma Stagnation in Inertial-Confinement Fusion. Physical Review Letters, 2012, 108, 025001.	7.8	27
256	Shock timing measurements and analysis in deuterium-tritium-ice layered capsule implosions on NIF. Physics of Plasmas, 2014, 21, 022703.	1.9	27
257	X-ray scattering measurements of dissociation-induced metallization of dynamically compressed deuterium. Nature Communications, 2016, 7, 11189.	12.8	27
258	Experimental results of radiation-driven, layered deuterium-tritium implosions with adiabat-shaped drives at the National Ignition Facility. Physics of Plasmas, 2016, 23, .	1.9	27
259	Hydro-instability growth of perturbation seeds from alternate capsule-support strategies in indirect-drive implosions on National Ignition Facility. Physics of Plasmas, 2017, 24, 102707.	1.9	27
260	Time-Resolved Fuel Density Profiles of the Stagnation Phase of Indirect-Drive Inertial Confinement Implosions. Physical Review Letters, 2020, 125, 155003.	7.8	27
261	<title>Gain uniformity, linearity, saturation, and depletion in gated microchannel-plate x-ray framing cameras</title> . , 1993, , .		26
262	Status of our understanding and modeling of x-ray coupling efficiency in laser heated hohlraums. Physics of Plasmas, 2001, 8, 260-265.	1.9	26
263	Plasma filling in reduced-scale hohlraums irradiated with multiple beam cones. Physics of Plasmas, 2006, 13, 112701.	1.9	26
264	First hohlraum drive studies on the National Ignition Facility. Physics of Plasmas, 2006, 13, 056315.	1.9	26
265	x-ray spectroscopic diagnostics of mix in high growth factor spherical implosions. Journal of Quantitative Spectroscopy and Radiative Transfer, 1995, 54, 207-220.	2.3	25
266	New methods for diagnosing and controlling hohlraum drive asymmetry on Nova. Physics of Plasmas, 1997, 4, 1862-1871.	1.9	25
267	Hydrodynamic instabilities seeded by the X-ray shadow of ICF capsule fill-tubes. Physics of Plasmas, 2018, 25, .	1.9	25
268	Hotspot parameter scaling with velocity and yield for high-adiabat layered implosions at the National Ignition Facility. Physical Review E, 2020, 102, 023210.	2.1	25
269	Yield and compression trends and reproducibility at NIF*. High Energy Density Physics, 2020, 36, 100755.	1.5	25
270	Using laser entrance hole shields to increase coupling efficiency in indirect drive ignition targets for the National Ignition Facility. Physics of Plasmas, 2006, 13, 056307.	1.9	24

#	Article	IF	CITATIONS
271	High order reflectivity of highly oriented pyrolytic graphite crystals for x-ray energies up to 22 keV. Review of Scientific Instruments, 2008, 79, 10E311.	1.3	24
272	Experimental validation of a diagnostic technique for tuning the fourth shock timing on National Ignition Facility. Physics of Plasmas, 2010, 17, 012703.	1.9	24
273	Observation of amplification of light by Langmuir waves and its saturation on the electron kinetic timescale. Journal of Plasma Physics, 2011, 77, 521-528.	2.1	24
274	Early time implosion symmetry from two-axis shock-timing measurements on indirect drive NIF experiments. Physics of Plasmas, 2014, 21, .	1.9	24
275	In-flight observations of low-mode <i>Ï</i> R asymmetries in NIF implosions. Physics of Plasmas, 2015, 22,	1.9	24
276	Fluence-compensated down-scattered neutron imaging using the neutron imaging system at the National Ignition Facility. Review of Scientific Instruments, 2016, 87, 11E715.	1.3	24
277	Design and performance of a high-power, synchronized Nd:YAG–dye laser system. Optics Letters, 1989, 14, 42.	3.3	23
278	Measurement of the Absolute Hohlraum-Wall Albedo under Ignition Foot Drive Conditions. Physical Review Letters, 2004, 93, 065002.	7.8	23
279	Laser coupling to reduced-scale hohlraum targets at the Early Light Program of the National Ignition Facility. Physics of Plasmas, 2005, 12, 056305.	1.9	23
280	Measurement of electron temperature of imploded capsules at the National Ignition Facility. Review of Scientific Instruments, 2012, 83, 10E121.	1.3	23
281	Progress toward ignition at the National Ignition Facility. Plasma Physics and Controlled Fusion, 2013, 55, 124015.	2.1	23
282	X-ray streaked refraction enhanced radiography for inferring inflight density gradients in ICF capsule implosions. Review of Scientific Instruments, 2018, 89, 10G108.	1.3	23
283	Hohlraum energetics and implosion symmetry with elliptical phase plates using a multi-cone beam geometry on OMEGA. Journal of Physics: Conference Series, 2008, 112, 022077.	0.4	22
284	Soft x-ray images of the laser entrance hole of ignition hohlraums. Review of Scientific Instruments, 2012, 83, 10E525.	1.3	22
285	Qualification of a high-efficiency, gated spectrometer for x-ray Thomson scattering on the National Ignition Facility. Review of Scientific Instruments, 2014, 85, 11D617.	1.3	22
286	X-ray area backlighter development at the National Ignition Facility (invited). Review of Scientific Instruments, 2014, 85, 11D502.	1.3	22
287	Visualizing deceleration-phase instabilities in inertial confinement fusion implosions using an "enhanced self-emission―technique at the National Ignition Facility. Physics of Plasmas, 2018, 25, 054502.	1.9	22
288	Integrated performance of large HDC-capsule implosions on the National Ignition Facility. Physics of Plasmas, 2020, 27, .	1.9	22

#	Article	IF	CITATIONS
289	Extensions of a classical mechanics "piston-model―for understanding the impact of asymmetry on ICF implosions: The cases of mode 2, mode 2/1 coupling, time-dependent asymmetry, and the relationship to coast-time. Physics of Plasmas, 2022, 29, .	1.9	22
290	Laser Scattering from Dense Cesium Plasmas. Physical Review Letters, 1985, 54, 1660-1663.	7.8	21
291	Experimental study of neutron induced background noise on gated x-ray framing cameras. Review of Scientific Instruments, 2010, 81, 10E515.	1.3	21
292	Areal density evolution of isolated surface perturbations at the onset of x-ray ablation Richtmyer-Meshkov growth. Physics of Plasmas, 2011, 18, .	1.9	21
293	Simulating x-ray Thomson scattering signals from high-density, millimetre-scale plasmas at the National Ignition Facility. Physics of Plasmas, 2014, 21, .	1.9	21
294	Gamma Reaction History ablator areal density constraints upon correlated diagnostic modeling of National Ignition Facility implosion experiments. Physics of Plasmas, 2015, 22, .	1.9	21
295	Hotspot electron temperature from x-ray continuum measurements on the NIF. Review of Scientific Instruments, 2016, 87, 11E534.	1.3	21
296	Mix and hydrodynamic instabilities on NIF. Journal of Instrumentation, 2017, 12, C06001-C06001.	1.2	21
297	Effects of asymmetry and hot-spot shape on ignition capsules. Physical Review E, 2018, 98, 023203.	2.1	21
298	Timeâ€resolved probing of femtosecondâ€laserâ€produced plasmas in transparent solids by electron thermal transport. Physics of Plasmas, 1995, 2, 476-485.	1.9	20
299	Effects of variable xâ€ray preheat shielding in indirectly driven implosions. Physics of Plasmas, 1996, 3, 2094-2097.	1.9	20
300	Hohlraum symmetry measurements with surrogate solid targets (invited). Review of Scientific Instruments, 1999, 70, 536-542.	1.3	20
301	The effect of shock dynamics on compressibility of ignition-scale National Ignition Facility implosions. Physics of Plasmas, 2014, 21, .	1.9	20
302	Observation of finite-wavelength screening in high-energy-density matter. Nature Communications, 2015, 6, 6839.	12.8	20
303	On krypton-doped capsule implosion experiments at the National Ignition Facility. Physics of Plasmas, 2017, 24, .	1.9	20
304	Heat transport modeling of the dot spectroscopy platform on NIF. Plasma Physics and Controlled Fusion, 2018, 60, 044009.	2.1	20
305	Review of hydro-instability experiments with alternate capsule supports in indirect-drive implosions on the National Ignition Facility. Physics of Plasmas, 2018, 25, 072705.	1.9	20
306	Achieving 280 Gbar hot spot pressure in DT-layered CH capsule implosions at the National Ignition Facility. Physics of Plasmas, 2020, 27, .	1.9	20

#	Article	IF	CITATIONS
307	Observation of Hydrodynamic Flows in Imploding Fusion Plasmas on the National Ignition Facility. Physical Review Letters, 2021, 127, 125001.	7.8	20
308	Indirectly driven, high growth Rayleigh-Taylor implosions on Nova. Journal of Quantitative Spectroscopy and Radiative Transfer, 1995, 54, 245-255.	2.3	19
309	Observation of reduced beam deflection using smoothed beams in gas-filled hohlraum symmetry experiments at Nova. Physics of Plasmas, 2000, 7, 1609-1613.	1.9	19
310	The size and structure of the laser entrance hole in gas-filled hohlraums at the National Ignition Facility. Physics of Plasmas, 2015, 22, .	1.9	19
311	Simulated performance of the optical Thomson scattering diagnostic designed for the National Ignition Facility. Review of Scientific Instruments, 2016, 87, 11E510.	1.3	19
312	Trending low mode asymmetries in NIF capsule drive using a simple viewfactor metric *. High Energy Density Physics, 2021, 40, 100944.	1.5	19
313	Diagnosis of pusherâ€fuel mix in spherical implosions using xâ€ray spectroscopy (invited). Review of Scientific Instruments, 1995, 66, 689-696.	1.3	18
314	10 and 5 μm pinhole-assisted point-projection backlit imaging for the National Ignition Facility. Review of Scientific Instruments, 2001, 72, 690-693.	1.3	18
315	First laser–plasma interaction and hohlraum experiments on the National Ignition Facility. Plasma Physics and Controlled Fusion, 2005, 47, B405-B417.	2.1	18
316	Empirical assessment of the detection efficiency of CR-39 at high proton fluence and a compact, proton detector for high-fluence applications. Review of Scientific Instruments, 2014, 85, 043302.	1.3	18
317	Performance and Mix Measurements of Indirect Drive Cu-Doped Be Implosions. Physical Review Letters, 2015, 114, 205002.	7.8	18
318	Application of cross-beam energy transfer to control drive symmetry in ICF implosions in low gas fill <i>Hohlraums</i> at the National Ignition Facility. Physics of Plasmas, 2020, 27, .	1.9	18
319	Highâ€resolution time―and twoâ€dimensional spaceâ€resolved xâ€ray imaging of plasmas at NOVA. Review of Scientific Instruments, 1992, 63, 5075-5078.	1.3	17
320	Direct Measurement of X-Ray Drive from Surrogate Targets in Nova Hohlraums. Physical Review Letters, 1996, 77, 3815-3818.	7.8	17
321	X-ray detection by direct modulation of an optical probe beam—Radsensor: Progress on development for imaging applications. Review of Scientific Instruments, 2004, 75, 3995-3997.	1.3	17
322	NIF-scale re-emission sphere measurements of early-time Tr=100eV hohlraum symmetry (invited). Review of Scientific Instruments, 2008, 79, 10E903.	1.3	17
323	Dense plasma X-ray scattering: Methods and applications. High Energy Density Physics, 2010, 6, 1-8.	1.5	17
324	Radiative shocks produced from spherical cryogenic implosions at the National Ignition Facility. Physics of Plasmas, 2013, 20, 056315.	1.9	17

#	Article	IF	CITATIONS
325	Hydrodynamic instability experiments with three-dimensional modulations at the National Ignition Facility. High Power Laser Science and Engineering, 2015, 3, .	4.6	17
326	A plasma amplifier to combine multiple beams at NIF. Physics of Plasmas, 2018, 25, .	1.9	17
327	First demonstration of improved capsule implosions by reducing radiation preheat in uranium vs gold hohlraums. Physics of Plasmas, 2018, 25, .	1.9	17
328	Production of dense, cool plasmas by resonance pumping of sodium vapor. Physical Review A, 1985, 32, 2963-2971.	2.5	16
329	Scaling of saturated stimulated Raman scattering with temperature and intensity in ignition scale plasmas. Physics of Plasmas, 2003, 10, 2948-2955.	1.9	16
330	Debris and shrapnel mitigation procedure for NIF experiments. Journal of Physics: Conference Series, 2008, 112, 032023.	0.4	16
331	Refraction-enhanced backlit imaging of axially symmetric inertial confinement fusion plasmas. Applied Optics, 2013, 52, 3538.	1.8	16
332	Observations of strong ion-ion correlations in dense plasmas. Physics of Plasmas, 2014, 21, 056302.	1.9	16
333	Using penumbral imaging to measure micrometer size plasma hot spots in Gbar equation of state experiments on the National Ignition Facility. Review of Scientific Instruments, 2014, 85, 11D614.	1.3	16
334	X-ray Thomson scattering as a temperature probe for Gbar shock experiments. Journal of Physics: Conference Series, 2014, 500, 192019.	0.4	16
335	Differential heating: A versatile method for thermal conductivity measurements in high-energy-density matter. Physics of Plasmas, 2015, 22, .	1.9	16
336	Shock Hugoniot measurements of CH at Gbar pressures at the NIF. Journal of Physics: Conference Series, 2016, 688, 012055.	0.4	16
337	Platform for spectrally resolved x-ray scattering from imploding capsules at the National Ignition Facility. Journal of Physics: Conference Series, 2016, 717, 012067.	0.4	16
338	Update 2015 on Target Fabrication Requirements for NIF Layered Implosions, with Emphasis on Capsule Support and Oxygen Modulations in GDP. Fusion Science and Technology, 2016, 70, 121-126.	1.1	16
339	Measurement of the local laser intensity by photoelectron energy shifts in multiphoton ionization. Journal of the Optical Society of America B: Optical Physics, 1989, 6, 344.	2.1	15
340	Preliminary performance measurements for a streak camera with a large-format direct-coupled charge-coupled device readout. Review of Scientific Instruments, 2004, 75, 4042-4044.	1.3	15
341	Observation of polarization dependent Raman scattering in a large scale plasma illuminated with multiple laser beams. Physics of Plasmas, 2006, 13, 082703.	1.9	15
342	Development of Compton radiography using high-Z backlighters produced by ultra-intense lasers. AIP Conference Proceedings, 2007, , .	0.4	15

#	Article	IF	CITATIONS
343	Influence and measurement of mass ablation in ICF implosions. Journal of Physics: Conference Series, 2008, 112, 022003.	0.4	15
344	Sensitivity of ignition scale backlit thin-shell implosions to hohlraum symmetry in the foot of the drive pulse. Physics of Plasmas, 2009, 16, .	1.9	15
345	X-ray streak camera cathode development and timing accuracy of the 4ï‰ ultraviolet fiducial system at the National Ignition Facility. Review of Scientific Instruments, 2012, 83, 10E123.	1.3	15
346	A compact proton spectrometer for measurement of the absolute DD proton spectrum from which yield and <i>ÏR</i> are determined in thin-shell inertial-confinement-fusion implosions. Review of Scientific Instruments, 2014, 85, 103504.	1.3	15
347	Kinetic mix mechanisms in shock-driven inertial confinement fusion implosions. Physics of Plasmas, 2014, 21, .	1.9	15
348	Calibration and characterization of a highly efficient spectrometer in von Hamos geometry for 7-10 keV x-rays. Review of Scientific Instruments, 2017, 88, 043110.	1.3	15
349	Simultaneous visualization of wall motion, beam propagation, and implosion symmetry on the National Ignition Facility (invited). Review of Scientific Instruments, 2018, 89, 10K111.	1.3	15
350	Development of new platforms for hydrodynamic instability and asymmetry measurements in deceleration phase of indirectly driven implosions on NIF. Physics of Plasmas, 2018, 25, 082705.	1.9	15
351	Evidence of restricted heat transport in National Ignition Facility Hohlraums. Physics of Plasmas, 2020, 27, 102704.	1.9	15
352	Hydro-scaling of direct-drive cylindrical implosions at the OMEGA and the National Ignition Facility. Physics of Plasmas, 2020, 27, 042708.	1.9	15
353	Low mode implosion symmetry sensitivity in low gas-fill NIF cylindrical hohlraums. Physics of Plasmas, 2021, 28, .	1.9	15
354	Exploring implosion designs for increased compression on the National Ignition Facility using high density carbon ablators. Physics of Plasmas, 2022, 29, .	1.9	15
355	Laser plasma diagnostics of dense plasmas. , 1995, , .		14
356	Indirect drive experiments utilizing multiple beam cones in cylindrical hohlraums on OMEGA. Physics of Plasmas, 1998, 5, 1960-1965.	1.9	14
357	X-ray induced pinhole closure in point-projection x-ray radiography. Journal of Applied Physics, 2006, 100, 043301.	2.5	14
358	Core temperature and density profile measurements in inertial confinement fusion implosions. High Energy Density Physics, 2008, 4, 1-17.	1.5	14
359	A diamond detector for X-ray bang-time measurement at the National Ignition Facility. Journal of Instrumentation, 2011, 6, P02009-P02009.	1.2	14
360	Raman Backscatter as a Remote Laser Power Sensor in High-Energy-Density Plasmas. Physical Review Letters, 2013, 111, 025001.	7.8	14

#	Article	IF	CITATIONS
361	Observation of strong electromagnetic fields around laser-entrance holes of ignition-scale hohlraums in inertial-confinement fusion experiments at the National Ignition Facility. New Journal of Physics, 2013, 15, 025040.	2.9	14
362	eHXI: a permanently installed, hard x-ray imager for the National Ignition Facility. Journal of Instrumentation, 2016, 11, P06010-P06010.	1.2	14
363	Maintaining low-mode symmetry control with extended pulse shapes for lower-adiabat Bigfoot implosions on the National Ignition Facility. Physics of Plasmas, 2019, 26, .	1.9	14
364	Understanding asymmetries using integrated simulations of capsule implosions in low gas-fill hohlraums at the National Ignition Facility. Plasma Physics and Controlled Fusion, 2021, 63, 025012.	2.1	14
365	Toroidally curved crystal for timeâ€resolved xâ€ray spectroscopy. Review of Scientific Instruments, 1985, 56, 803-805.	1.3	13
366	Xâ€ray framing camera for picosecond imaging of laserâ€produced plasmas. Review of Scientific Instruments, 1989, 60, 363-367.	1.3	13
367	Recent progress in high-energy, high-resolution x-ray imaging techniques for application to the National Ignition Facility (invited). Review of Scientific Instruments, 1999, 70, 525-529.	1.3	13
368	Role of laser beam geometry in improving implosion symmetry and performance for indirect-drive inertial confinement fusion. Physics of Plasmas, 2003, 10, 2429-2432.	1.9	13
369	Characterization of the series 1000 camera system. Review of Scientific Instruments, 2004, 75, 4060-4062.	1.3	13
370	Gas-filled hohlraum experiments at the National Ignition Facility. Physics of Plasmas, 2006, 13, 056319.	1.9	13
371	Experimental studies of ICF indirect-drive Be and high density C candidate ablators. Journal of Physics: Conference Series, 2008, 112, 022004.	0.4	13
372	X-ray Thomson scattering measurements of temperature and density from multi-shocked CH capsules. Physics of Plasmas, 2013, 20, .	1.9	13
373	High energy xâ€ray imaging diagnostic on Nova. Review of Scientific Instruments, 1992, 63, 5083-5085.	1.3	12
374	Prospects for fluorescence based imaging/visualization of hydrodynamic systems on the National Ignition Facility. Review of Scientific Instruments, 1999, 70, 663-666.	1.3	12
375	Thinshell symmetry surrogates for the National Ignition Facility: A rocket equation analysis. Physics of Plasmas, 2001, 8, 2908-2917.	1.9	12
376	Limits on collective X-ray scattering imposed by coherence. Europhysics Letters, 2006, 74, 637-643.	2.0	12
377	Pressure-driven, resistive magnetohydrodynamic interchange instabilities in laser-produced high-energy-density plasmas. Physical Review E, 2009, 80, 016407.	2.1	12
378	Prediction of ignition implosion performance using measurements of Low-deuterium surrogates. Journal of Physics: Conference Series, 2010, 244, 022014.	0.4	12

#	Article	IF	CITATIONS
379	Observations of multimode perturbation decay at non-accelerating, soft x-ray driven ablation fronts. Physics of Plasmas, 2012, 19, .	1.9	12
380	A magnetic particle time-of-flight (MagPTOF) diagnostic for measurements of shock- and compression-bang time at the NIF (invited). Review of Scientific Instruments, 2014, 85, 11D901.	1.3	12
381	Simulations of indirectly driven gas-filled capsules at the National Ignition Facility. Physics of Plasmas, 2014, 21, .	1.9	12
382	Indirect-drive ablative Richtmyer Meshkov node scaling. Journal of Physics: Conference Series, 2016, 717, 012034.	0.4	12
383	Images of the gold bubble feature in NIF Gas-Filled Ignition Hohlraums. Journal of Physics: Conference Series, 2016, 717, 012049.	0.4	12
384	Semi-empirical "leaky-bucket―model of laser-driven x-ray cavities. Physics of Plasmas, 2017, 24, .	1.9	12
385	Experimental demonstration of the reduced expansion of a laser-heated surface using a low density foam layer, pertaining to advanced hohlraum designs with less wall-motion. Physics of Plasmas, 2020, 27, .	1.9	12
386	Three dimensional low-mode areal-density non-uniformities in indirect-drive implosions at the National Ignition Facility. Physics of Plasmas, 2021, 28, .	1.9	12
387	Optimized continuum x-ray emission from laser-generated plasma. Applied Physics Letters, 2020, 117, .	3.3	12
388	Electrical characteristics of short pulse gated microchannel plate detectors. Review of Scientific Instruments, 1992, 63, 5072-5074.	1.3	11
389	Lawrence Livermore National Laboratory's activities to achieve ignition by X-ray drive on the National Ignition Facility. Laser and Particle Beams, 1999, 17, 159-171.	1.0	11
390	The first target experiments on the National Ignition Facility. European Physical Journal D, 2007, 44, 273-281.	1.3	11
391	Observation of hohlraum-wall motion with spectrally selective x-ray imaging at the National Ignition Facility. Review of Scientific Instruments, 2016, 87, 11E321.	1.3	11
392	The preliminary design of the optical Thomson scattering diagnostic for the National Ignition Facility. Journal of Physics: Conference Series, 2016, 717, 012089.	0.4	11
393	Fill tube dynamics in inertial confinement fusion implosions with high density carbon ablators. Physics of Plasmas, 2020, 27, .	1.9	11
394	Carbon ablator areal density at fusion burn: Observations and trends at the National Ignition Facility. Physics of Plasmas, 2020, 27, .	1.9	11
395	Fuel convergence sensitivity in indirect drive implosions. Physics of Plasmas, 2021, 28, 042705.	1.9	11
396	Time-resolved X-ray spectroscopy of deeply buried tracer layers as a density and temperature diagnostic for the fast ignitor. Laser and Particle Beams, 1998, 16, 225-232.	1.0	10

#	Article	IF	CITATIONS
397	Turbulent hydrodynamics experiments using a new plasma piston. Physics of Plasmas, 2000, 7, 2099-2107.	1.9	10
398	Comparison of charge coupled device vs film readouts for gated micro-channel plate cameras. Review of Scientific Instruments, 2001, 72, 706-708.	1.3	10
399	Saturation of power transfer between two copropagating laser beams by ion-wave scattering in a single-species plasma. Physics of Plasmas, 2005, 12, 112701.	1.9	10
400	Hard x-ray imaging for measuring laser absorption spatial profiles on the National Ignition Facility. Review of Scientific Instruments, 2006, 77, 10E310.	1.3	10
401	Diagnosing ablator ÏR and ÏR asymmetries in capsule implosions using charged-particle spectrometry at the National Ignition Facility. Physics of Plasmas, 2009, 16, 022702.	1.9	10
402	Assessment and mitigation of radiation, EMP, debris & shrapnel impacts at megajoule-class laser facilities. Journal of Physics: Conference Series, 2010, 244, 032018.	0.4	10
403	AXIS: An instrument for imaging Compton radiographs using the Advanced Radiography Capability on the NIF. Review of Scientific Instruments, 2014, 85, 11D624.	1.3	10
404	Improving the off-axis spatial resolution and dynamic range of the NIF X-ray streak cameras (invited). Review of Scientific Instruments, 2016, 87, 11E202.	1.3	10
405	Simplified model of pinhole imaging for quantifying systematic errors in image shape. Applied Optics, 2017, 56, 8719.	1.8	10
406	Hydrodynamic instability seeding by oxygen nonuniformities in glow discharge polymer inertial fusion ablators. Physical Review E, 2018, 98, .	2.1	10
407	Experimental study of atomic structure in strong electromagnetic fields. Physical Review A, 1989, 40, 2766-2769.	2.5	9
408	An assessment of the 3D geometric surrogacy of shock timing diagnostic techniques for tuning experiments on the NIF. Journal of Physics: Conference Series, 2008, 112, 022078.	0.4	9
409	Lasnex simulations of NIF vacuum hohlraum commissioning experiments. Journal of Physics: Conference Series, 2010, 244, 032057.	0.4	9
410	Laser absorption, power transfer, and radiation symmetry during the first shock of inertial confinement fusion gas-filled hohlraum experiments. Physics of Plasmas, 2015, 22, 122701.	1.9	9
411	Capsule Ablator Inflight Performance Measurements Via Streaked Radiography Of ICF Implosions On The NIF*. Journal of Physics: Conference Series, 2016, 688, 012014.	0.4	9
412	A direct-drive exploding-pusher implosion as the first step in development of a monoenergetic charged-particle backlighting platform at the National Ignition Facility. High Energy Density Physics, 2016, 18, 38-44.	1.5	9
413	View factor estimation of hot spot velocities in inertial confinement fusion implosions at the National Ignition Facility. Physics of Plasmas, 2020, 27, .	1.9	9
414	First study of Hohlraum x-ray preheat asymmetry inside an ICF capsule. Physics of Plasmas, 2020, 27, 122703.	1.9	9

#	Article	IF	CITATIONS
415	Induced frequency shifts by counterpropagating subpicosecond optical pulses. Optics Letters, 1993, 18, 723.	3.3	8
416	Time-resolved backside optical probing of picosecond-laser-pulse-produced plasma in solid materials. Physical Review E, 1993, 47, 2768-2777.	2.1	8
417	A comparative study of x-ray emission from laser spots in laser-heated hohlraums relative to spots on simple disk targets. Physics of Plasmas, 1997, 4, 778-787.	1.9	8
418	Towards a complete model of 3D line emission from ICF capsules: results from the first 3D simulations. Journal of Quantitative Spectroscopy and Radiative Transfer, 2000, 65, 353-366.	2.3	8
419	Modeling titanium line emission from ICF capsules in three dimensions. Journal of Quantitative Spectroscopy and Radiative Transfer, 2001, 71, 479-492.	2.3	8
420	Comparisons of line emission from 2- and 3-dimensionsal simulations of ICF capsules to experiments. Journal of Quantitative Spectroscopy and Radiative Transfer, 2003, 81, 275-286.	2.3	8
421	RadSensor: x-ray detection by direct modulation of an optical probe beam. , 2004, , .		8
422	Ultrafast Kα x-ray Thomson scattering from shock compressed lithium hydride. Physics of Plasmas, 2009, 16, 056308.	1.9	8
423	NIF unconverted light and its influence on DANTE measurements. Review of Scientific Instruments, 2009, 80, 063104.	1.3	8
424	First hot electron measurements in near-ignition scale hohlraums on the National Ignition Facility. Journal of Physics: Conference Series, 2010, 244, 022074.	0.4	8
425	Development of X-ray Thomson scattering for implosion target characterization. High Energy Density Physics, 2011, 7, 271-276.	1.5	8
426	Amplification of light in a plasma by stimulated ion acoustic waves driven by multiple crossing pump beams. Physical Review E, 2011, 84, 026402.	2.1	8
427	Instruments, 2012, 83, 10D310.	1.3	8
428	Hard x-ray (>100 keV) imager to measure hot electron preheat for indirectly driven capsule implosions on the NIF. Review of Scientific Instruments, 2012, 83, 10E508.	1.3	8
429	Development of a dual MCP framing camera for high energy x-rays. Review of Scientific Instruments, 2014, 85, 11D623.	1.3	8
430	A simulation-based model for understanding the time dependent x-ray drive asymmetries and error bars in indirectly driven implosions on the National Ignition Facility. Physics of Plasmas, 2019, 26, 062703.	1.9	8
431	Optimization of high energy x ray production through laser plasma interaction. High Energy Density Physics, 2019, 31, 13-18.	1.5	8
432	Recent and planned hydrodynamic instability experiments on indirect-drive implosions on the National Ignition Facility. High Energy Density Physics, 2020, 36, 100820.	1.5	8

#	Article	IF	CITATIONS
433	Demonstration of a laser-driven, narrow spectral bandwidth x-ray source for collective x-ray scattering experiments. Physics of Plasmas, 2021, 28, .	1.9	8
434	Testing quantum mechanics in non-Minkowski space-time with high power lasers and 4th generation light sources. Scientific Reports, 2012, 2, 491.	3.3	8
435	Design of Cylindrical Implosion Experiments to Demonstrate Scale-Invariant Rayleigh-Taylor Instability Growth. High Energy Density Physics, 2020, 36, 100831.	1.5	8
436	Detailed measurements and shaping of gate profiles for microchannel-plate-based x-ray framing cameras. , 1994, , .		7
437	X-ray diagnostics of hohlraum plasma flow. Review of Scientific Instruments, 1997, 68, 831-833.	1.3	7
438	Relative x-ray backlighter intensity comparison of Ti and Ti/Sc combination foils driven in double-sided and single-sided laser configuration. Review of Scientific Instruments, 2001, 72, 686-689.	1.3	7
439	Tracer spectroscopy diagnostics of doped ablators in inertial confinement fusion experiments on OMEGA. Physics of Plasmas, 2004, 11, 2702-2708.	1.9	7
440	Solid-density plasma characterization with x-ray scattering on the 200J Janus laser. Review of Scientific Instruments, 2006, 77, 10F317.	1.3	7
441	Diagnosing indirect-drive inertial-confinement-fusion implosions with charged particles. Plasma Physics and Controlled Fusion, 2010, 52, 124027.	2.1	7
442	Developing a bright 17 keV x-ray source for probing high-energy-density states of matter at high spatial resolution. Physics of Plasmas, 2015, 22, 043114.	1.9	7
443	Using neutrons to measure keV temperatures in highly compressed plastic at multi-Gbar pressures. High Energy Density Physics, 2016, 21, 20-26.	1.5	7
444	Measurements of enhanced performance in an indirect drive inertial confinement fusion experiment when reducing the contact area of the capsule support. Physics of Plasmas, 2020, 27, .	1.9	7
445	Time resolved ablator areal density during peak fusion burn on inertial confinement fusion implosions. Physics of Plasmas, 2021, 28, 032701.	1.9	7
446	Metrics for implosion performance with enhanced energy coupling on NIF. Nuclear Fusion, 2021, 61, 116066.	3.5	7
447	Proton imaging of hohlraum plasma stagnation in inertial-confinement-fusion experiments. Nuclear Fusion, 2013, 53, 073022.	3.5	7
448	X-ray penumbral imaging diagnostic developments at the National Ignition Facility. , 2017, , .		7
449	Investigation of quantum efficiencies in multilayered photocathodes for microchannel plate applications. Review of Scientific Instruments, 1999, 70, 659-662.	1.3	6
450	Static and time-resolved 10–1000â€,keV x-ray imaging detector options for NIF. Review of Scientific Instruments, 2004, 75, 4037-4039.	1.3	6

#	Article	IF	CITATIONS
451	The effect of condensates and inner coatings on the performance of vacuum hohlraum targets. Physics of Plasmas, 2010, 17, 032701.	1.9	6
452	Simple solution to the Fresnel–Kirchoff diffraction integral for application to refraction-enhanced radiography. Journal of the Optical Society of America A: Optics and Image Science, and Vision, 2013, 30, 1460.	1.5	6
453	Early-time radiation flux symmetry optimization and its effect on gas-filled hohlraum ignition targets on the National Ignition Facility. Physics of Plasmas, 2016, 23, .	1.9	6
454	X-ray Thomson scattering measurements from hohlraum-driven spheres on the OMEGA laser. Review of Scientific Instruments, 2016, 87, 11E724.	1.3	6
455	The design of the optical Thomson scattering diagnostic for the National Ignition Facility. Review of Scientific Instruments, 2016, 87, 11E549.	1.3	6
456	Improving a high-efficiency, gated spectrometer for x-ray Thomson scattering experiments at the National Ignition Facility. Review of Scientific Instruments, 2016, 87, 11E515.	1.3	6
457	Direct observation of density gradients in ICF capsule implosions via streaked Refraction Enhanced Radiography (RER). High Energy Density Physics, 2020, 36, 100795.	1.5	6
458	The effects of multispecies <i>Hohlraum</i> walls on stimulated Brillouin scattering, <i>Hohlraum</i> dynamics, and beam propagation. Physics of Plasmas, 2021, 28, .	1.9	6
459	Production of dense, cool plasmas by multiphoton ionization of sodium vapor. Physical Review A, 1985, 32, 2972-2976.	2.5	5
460	An xâ€ray technique for precision laser beam synchronization. Review of Scientific Instruments, 1995, 66, 788-790.	1.3	5
461	Yield and emission line ratios from ICF target implosions with multi-mode Rayleigh-Taylor perturbations. Journal of Quantitative Spectroscopy and Radiative Transfer, 1997, 58, 709-720.	2.3	5
462	Compton scattering measurements from dense plasmas*. Journal of Physics: Conference Series, 2008, 112, 032071.	0.4	5
463	Study of direct-drive capsule implosions in inertial confinement fusion with proton radiography. Plasma Physics and Controlled Fusion, 2009, 51, 014003.	2.1	5
464	X-ray continuum emission spectroscopy from hot dense matter at Gbar pressures. Review of Scientific Instruments, 2014, 85, 11D606.	1.3	5
465	Using time-resolved penumbral imaging to measure low hot spot x-ray emission signals from capsule implosions at the National Ignition Facility. Review of Scientific Instruments, 2018, 89, 10G111.	1.3	5
466	Implementing time resolved electron temperature capability at the NIF using a streak camera. Review of Scientific Instruments, 2018, 89, 10K117.	1.3	5
467	Inference of the electron temperature in inertial confinement fusion implosions from the hard Xâ€ray spectral continuum. Contributions To Plasma Physics, 2019, 59, 181-188.	1.1	5
468	Optimization of capsule dopant levels to improve fuel areal density*. High Energy Density Physics, 2020, 37, 100884.	1.5	5

#	Article	IF	CITATIONS
469	Symmetry tuning and high energy coupling for an Al capsule in a Au rugby hohlraum on NIF. Physics of Plasmas, 2020, 27, .	1.9	5
470	<title>X-ray framing cameras for >5 keV imaging</title> . , 1995, , .		4
471	X-ray Thomson scattering for measuring dense beryllium plasma collisionality. Journal of Physics: Conference Series, 2010, 244, 032044.	0.4	4
472	Experimental evaluation of neutron induced noise on gated x-ray framing cameras. Journal of Physics: Conference Series, 2010, 244, 032048.	0.4	4
473	Measurements of hohlraum-produced fast ions. Physics of Plasmas, 2012, 19, .	1.9	4
474	Adiabatic Index in Shock ompressed Beryllium. Contributions To Plasma Physics, 2012, 52, 186-193.	1.1	4
475	Structured photocathodes for improved high-energy x-ray efficiency in streak cameras. Review of Scientific Instruments, 2016, 87, 11E331.	1.3	4
476	Improved hard x-ray (50-80 keV) imaging of hohlraum implosion experiments at the National Ignition Facility. Proceedings of SPIE, 2016, , .	0.8	4
477	Developing a long-duration Zn K-α source for x-ray scattering experiments. Review of Scientific Instruments, 2018, 89, 10F109.	1.3	4
478	Developing "inverted-corona―fusion targets as high-fluence neutron sources. Review of Scientific Instruments, 2021, 92, 033544.	1.3	4
479	Toward an integrated platform for characterizing laser-driven, isochorically heated plasmas with 1  µm spatial resolution. Applied Optics, 2022, 61, 1987.	1.8	4
480	Hydroscaling indirect-drive implosions on the National Ignition Facility. Physics of Plasmas, 2022, 29, .	1.9	4
481	Photoconductive measurements on microwave-assisted plasma-enhanced chemically vapor deposited diamond films. Surface and Coatings Technology, 1991, 47, 356-364.	4.8	3
482	<title>Multiframe x-ray imaging with a large-area 40ps camera</title> . , 1993, 1757, 93.		3
483	Implosions: An Experimental Testbed for Highâ€Energy Density Physics. Astrophysical Journal, Supplement Series, 2000, 127, 227-232.	7.7	3
484	<title>Multi-kilovolt x-ray conversion efficiencies</title> ., 2001, 4504, 133.		3
485	Shielding a streak camera from hard x rays. Review of Scientific Instruments, 2004, 75, 4040-4041.	1.3	3
486	Design of a streaked radiography instrument for ICF ablator tuning measurements. Review of Scientific Instruments, 2008, 79, 10E913.	1.3	3

#	Article	IF	CITATIONS
487	Development of a Laser-Produced Plasma X-Ray Source for Phase-Contrast Radiography of D-T Ice Layers. Fusion Science and Technology, 2009, 55, 253-259.	1.1	3
488	Diagnosing implosions at the national ignition facility with X-ray spectroscopy. AIP Conference Proceedings, 2012, , .	0.4	3
489	Improved modeling of microchannel plate response to hard X-rays. Nuclear Instruments and Methods in Physics Research, Section A: Accelerators, Spectrometers, Detectors and Associated Equipment, 2013, 705, 17-23.	1.6	3
490	Design calculations for NIF convergent ablator experiments. EPJ Web of Conferences, 2013, 59, 02008.	0.3	3
491	High quantum efficiency photocathode simulation for the investigation of novel structured designs. Review of Scientific Instruments, 2014, 85, 11D625.	1.3	3
492	Hydrodynamic growth experiments with the 3-D, "native-roughness―modulations on NIF. Journal of Physics: Conference Series, 2016, 717, 012052.	0.4	3
493	Hydrodynamic instabilities and mix studies on NIF: predictions, observations, and a path forward. Journal of Physics: Conference Series, 2016, 688, 012090.	0.4	3
494	Spatial resolution measurements of the advanced radiographic capability x-ray imaging system at energies relevant to Compton radiography. Review of Scientific Instruments, 2016, 87, 11E310.	1.3	3
495	Hydrodynamic growth and mix experiments at National Ignition Facility. Journal of Physics: Conference Series, 2016, 688, 012113.	0.4	3
496	Applications and results of X-ray spectroscopy in implosion experiments on the National Ignition Facility. AIP Conference Proceedings, 2017, , .	0.4	3
497	Positron radiography of ignition-relevant ICF capsules. Physics of Plasmas, 2017, 24, .	1.9	3
498	Influence of argon impurities on the elastic scattering of x-rays from imploding beryllium capsules. High Energy Density Physics, 2018, 26, 86-92.	1.5	3
499	Measurements of gas filled halfraum energetics at the national ignition facility using a single quad. European Physical Journal Special Topics, 2006, 133, 919-923.	0.2	3
500	X-ray flux and X-ray burnthrough experiments on reduced-scale targets at the NIF and OMEGA lasers. European Physical Journal Special Topics, 2006, 133, 1205-1208.	0.2	3
501	A study of space charge induced non-linearity in the Single Line Of Sight camera. Review of Scientific Instruments, 2022, 93, 023505.	1.3	3
502	Anomalous Cs I 5d-5⨕lineshape in a non-debye plasma. Journal of Quantitative Spectroscopy and Radiative Transfer, 1985, 34, 177-182.	2.3	2
503	Transient photoconductive measurements of microwave and DC plasma CVD produced diamond films. Carbon, 1990, 28, 791.	10.3	2
504	Ultrafast gain quenching in laser amplifiers. Optics Letters, 1991, 16, 590.	3.3	2

#	Article	IF	CITATIONS
505	Hydrodynamic evolution of picosecond laser plasmas. , 1991, 1413, 120.		2
506	Sub-100 psec x-ray gating cameras for ICF imaging applications. , 1991, , .		2
507	High-energy x-ray source generation by short-pulse high-intensity lasers. , 2004, , .		2
508	High-energy density science with FELs: intense short pulse tunable X-ray sources. , 2006, 6261, 626101.		2
509	X-ray Thomson scattering measurement in shock-compressed beryllium. Journal of Physics: Conference Series, 2010, 244, 042015.	0.4	2
510	Hohlraum designs for high velocity implosions on NIF. EPJ Web of Conferences, 2013, 59, 02002.	0.3	2
511	Design calculations for a xenon plasma x-ray shield to protect the NIF optical Thomson scattering diagnostic. Review of Scientific Instruments, 2016, 87, 11D603.	1.3	2
512	Measurement of inflight shell areal density near peak velocity using a self backlighting technique. Journal of Physics: Conference Series, 2016, 717, 012044.	0.4	2
513	Advances in shock timing experiments on the National Ignition Facility. Journal of Physics: Conference Series, 2016, 688, 012092.	0.4	2
514	Initial experimental demonstration of the principles of a xenon gas shield designed to protect optical components from soft x-ray induced opacity (blanking) in high energy density experiments. Physics of Plasmas, 2017, 24, 032705.	1.9	2
515	Update 2017 on Target Fabrication Requirements for High-Performance NIF Implosion Experiments. Fusion Science and Technology, 2018, 73, 83-88.	1.1	2
516	Alternative irradiation schemes for NIF and LMJ hohlraums. Plasma Physics and Controlled Fusion, 2018, 60, 025006.	2.1	2
517	A novel method to measure ion density in ICF experiments using x-ray spectroscopy of cylindrical tracers. Physics of Plasmas, 2020, 27, 112714.	1.9	2
518	Foam-lined hohlraum, inertial confinement fusion experiments on the National Ignition Facility. Physical Review E, 2020, 102, 051201.	2.1	2
519	Absorption spectroscopy of a laserâ€produced plasma. Review of Scientific Instruments, 1986, 57, 2197-2197.	1.3	1
520	Review of Drive Symmetry Measurement and Control Experiments on the Nova Laser System. Fusion Science and Technology, 1994, 26, 687-695.	0.6	1
521	Production of multikilovolt x rays from laser-heated targets. , 1997, 3157, 130.		1
522	Imaging detectors for 20–100â€,keV x-ray backlighters in high-energy-density experimental science petawatt experiments. Review of Scientific Instruments, 2004, 75, 4051-4053.	1.3	1

#	Article	IF	CITATIONS
523	Studies of background levels for the NIF yield diagnostics from neutron and gamma radiation. Journal of Physics: Conference Series, 2008, 112, 032083.	0.4	1
524	Inferring the electron temperature and density of shocked liquid deuterium using inelastic X-ray scattering. Journal of Physics: Conference Series, 2010, 244, 042017.	0.4	1
525	Symmetry tuning with megajoule laser pulses at the National Ignition Facility. EPJ Web of Conferences, 2013, 59, 02007.	0.3	1
526	Ignition tuning for the National Ignition Campaign. EPJ Web of Conferences, 2013, 59, 01003.	0.3	1
527	Shock timing on the National Ignition Facility: First experiments. EPJ Web of Conferences, 2013, 59, 02004.	0.3	1
528	Shock timing on the National Ignition Facility: The first precision tuning series. EPJ Web of Conferences, 2013, 59, 02005.	0.3	1
529	Precision fabrication of large area silicon-based geometrically enhanced x-ray photocathodes using plasma etching. Proceedings of SPIE, 2015, , .	0.8	1
530	Measurement of hydrodynamic instability growth during the deceleration of an inertial confinement fusion implosion. High Energy Density Physics, 2020, 37, 100817.	1.5	1
531	Hohlraum x-ray preheat asymmetry measurement at the ICF capsule via Mo ball fluorescence imaging. Review of Scientific Instruments, 2021, 92, 023517.	1.3	1
532	The first experiments on the national ignition facility. European Physical Journal Special Topics, 2006, 133, 43-45.	0.2	1
533	Using neutrons and x rays to measure plasma conditions in a solid sphere of deuterated polyethylene compressed to densities of 35 g/cc at temperatures of 2 keV and pressures of 40 Gbar. Physics of Plasmas, 2021, 28, .	1.9	1
534	<title>Laser frequency shifts in picosecond laser-produced plasmas</title> . , 1990, 1229, 107.		0
535	Recent Nova Experimental Results. Fusion Science and Technology, 1992, 21, 1340-1343.	0.6	Ο
536	Precision operation of the Nova laser for fusion experiments. AIP Conference Proceedings, 1994, , .	0.4	0
537	Neutron detectors for fusion reaction-rate measurements. AIP Conference Proceedings, 1994, , .	0.4	Ο
538	Implementation of 40-ps high-speed-gated microchannel-plate-based x-ray framing cameras on reentrant SIMs for Nova. , 1994, , .		0
539	Temporally and radially-resolved femtosecond optical measurements of solid density plasma reflectivities and transmissivities. Journal of Quantitative Spectroscopy and Radiative Transfer, 1995, 54, 413-418.	2.3	0
540	Shock physics with the nova laser for icf applications. AIP Conference Proceedings, 1996, , .	0.4	0

#	Article	IF	CITATIONS
541	Atomic processes in inertial fusion plasmas. , 1998, , .		0
542	Diagnosing plasma gradients using spectral line shapes. AIP Conference Proceedings, 2001, , .	0.4	0
543	<title>Warm dense plasma characterization by x-ray Thomson scattering</title> . , 2001, , .		0
544	<title>Symmetry experiments on Omega with LMJ-like multiple beam cone irradiation</title> .,2001, 4424,23.		0
545	Calculations and measurements of x-ray Thomson scattering spectra in warm dense matter. AIP Conference Proceedings, 2002, , .	0.4	0
546	Target diagnostic technology research and development for the LLNL ICF and HED program (invited). Review of Scientific Instruments, 2004, 75, 4200-4203.	1.3	0
547	Impact of neutron and gamma radiation on the design of NIF diagnostics and target-bay systems. European Physical Journal Special Topics, 2006, 133, 907-912.	0.2	0
548	Hard X-ray and hot electron environment in vacuum hohlraums at NIF. European Physical Journal Special Topics, 2006, 133, 313-315.	0.2	0
549	Capsule performance optimization in the national ignition campaign. Journal of Physics: Conference Series, 2010, 244, 022004.	0.4	0
550	3D Simulations of the NIF indirect drive ignition target design. Journal of Physics: Conference Series, 2010, 244, 022077.	0.4	0
551	Publisher's Note: Demonstration of Ignition Radiation Temperatures in Indirect-Drive Inertial Confinement Fusion Hohlraums [Phys. Rev. Lett.106, 085004 (2011)]. Physical Review Letters, 2011, 106, .	7.8	0
552	Measurements of the properties of highly compressed degenerate matter using X-ray Thomson scattering. , 2012, , .		0
553	X-ray Thomson scattering measurements from shock-compressed deuterium. , 2012, , .		0
554	M-ARIANE (Mirror-assisted Active Readout In A Neutron Environment): an x-ray imaging system for implosion experiments on the National Ignition Facility at ignition neutron yields. , 2013, , .		0
555	Bump evolution driven by the x-ray ablation Richtmyer-Meshkov effect in plastic inertial confinement fusion Ablators. EPJ Web of Conferences, 2013, 59, 04003.	0.3	0
556	Reproducibility of hohlraum-driven implosion symmetry on the National Ignition Facility. EPJ Web of Conferences, 2013, 59, 02010.	0.3	0
557	Demonstration of enhanced DQE with a dual MCP configuration. , 2014, , .		0
558	Performance of indirectly driven capsule implosions on NIF using adiabat-shaping. Journal of Physics: Conference Series, 2016, 717, 012045.	0.4	0

#	Article	IF	CITATIONS
559	Imploded capsule fuel temperature and density measurement by energy-dependent neutron imaging. European Physical Journal Special Topics, 2006, 133, 925-927.	0.2	Ο
560	Laser coupling to reduced-scale targets at NIF Early Light. European Physical Journal Special Topics, 2006, 133, 237-241.	0.2	0
561	Development of slit projection radiography with $1 \hat{A} \mu m$ resolution at the Omega Laser Facility. , 2021, , .		Ο
562	Measuring Dynamic Density Gradients in Warm Dense Matter with 1 ŵm Spatial Resolution. , 2021, , .		0
563	Fresnel Diffractive Radiography Measurements of Transport Properties in Warm Dense Matter. , 2022, ,		0